Reduced active area in transition-edge sensors for visible-NIR photon detection: A comparison of experimental data and two-fluid model

Reduced active area in transition-edge sensors for visible-NIR photon detection: a comparison of experimental data and two-fluid model

E. Taralli, L. Lolli, C. Portesi, E. Monticone, M. Rajteri,T-S Wang, J-K Chen, and X. Zhou

***Abstract*—Transition-Edge Sensors (TESs) are very versatile superconducting devices used to detect radiation from gamma-rays to visible and submillimeter. The intrinsic capability to measure the energy of the absorbed photons with very high energy resolution and the related possibility to resolve the number of incident photons distinguish photon-number resolving (PNR) devices from any other photon detectors. PNR detectors are fundamental for the measurement of the photon-number distribution of single-photon emitters and for the progress of quantum information technology and quantum metrology.**

By reducing the active area of TESs for visible-NIR light from typical values of 10^{-10} m^2 toward 10^{-12} m^2 and by increasing the TES operating temperature, we should be able to combine the high energy resolution permitted by very low heat capacity with fast response time. In order to support the future design and development of this new type of detector, in this work we compare experimental data with circuit simulation results based on the two-fluid theory.

***Index Terms*— Device modeling, Superconducting devices, Superconducting thin films,Transition-edge sensor.**

I. Introduction

THE explosive growth, over the last few decades, of quantum-information science and quantum optics [1,2] has been possible thanks to the progress in single photon generation, detection and manipulation. Among single photon detectors, transition-edge sensors (TESs) are the only one intrinsically able to resolve the number of photons in a light pulse (knowing the incident photon wavelength), or to measure the energy of the incident photons. The development of photon-number-resolving (PNR) TESs is important for applications that range from quantum communication [3], and astronomy [4], to material analysis [5] and quantum metrology [6-7].

Moreover the development of fast PNR detectors with high counting rates (>500 kHz) is fundamental to optical quantum computing [8] and quantum key distribution (QKD) [9].

The most common design requirements for single-photon detectors are high energy resolution (ΔE), 100% of quantum efficiency (QE), negligible dark-counts rate, low time jitter and fast response time. Unfortunately, these parameters are not independent and the design is usually a compromise. For instance, ΔE and effective response time (τ_{eff}) are directly and inversely proportional to the superconducting transition temperature (T_c), respectively.

In this paper we present TESs with active areas less than 5 μm^2 that use titanium as the superconducting material. We compare experimental data to simulation results with the goal of validating the two-fluid theory for these small Ti-based TESs. These reduced dimensions could lead to size-effects that are not significant in larger areas TES, such as the weak-link behavior [10] and the proximity effect between the Nb wiring and the Ti layer. Therefore it is interesting to investigate whether the two-fluid model is still valid for our smaller devices and whether we can also describe some of the general trends that are observed in traditional TESs.

II. Devices and Parameters Optimization

So far, TESs have been fabricated using different superconducting materials. Tungsten-based TESs with an area of 18 µm × 18 µm have reached an excellent energy resolution ΔE=0.12 eV with a slow response time of 30 µs [11], whereas titanium-based 5 µm × 5 µm TESs have achieved a fast response time τ_{eff}= 190 ns with an energy resolution of 0.39 eV [12]. Titanium superconducting hot-electron microcalorimeter have achieved ΔE=0.11 eV, but again a slow response time (~10µs) [13]. In titanium-gold based 10 µm × 10 µm TESs [14], the Au thickness can be varied to tune the device properties to obtain detectors with very high energy resolution (ΔE=0.113±0.001 eV, T_c=106mK) [15] or with fast response time (τ_{eff}= 186 ns, T_c=301.5mK) [16].

The real challenge is to design and fabricate TESs with optimized energy resolution and response time simultaneously. As is well known from the TES theory [17], in the spectral range from optical to near-infrared, the absorbed photons directly heat the electronic system of the metal film. The TES temperature increases by $\Delta T = E_\gamma/C_e$ where E_γ is the energy of the impinging photon and $C_e(\propto T_c)$ is the electronic heat

Manuscript received August 12, 2014. This research receives funding from the European Community's Seventh Framework Programme, ERA-NET Plus, under Grant Agreement No. 912/2009/EC..

E. Taralli, L. Lolli, C. Portesi, E. Monticone and M. Rajteri are with Istituto Nazionale di Ricerca Metrologica INRIM, 10135 Torino, Italy. Corresponding author E. Taralli: 0039-0113919220; fax: 0039-011346384; e-mail: e.taralli@inrim.it.

T-S. Wang, J-K. Chen, and X. Zhou are with the Department of Optics and Optical Engineering, the CAS Laboratory of Quantum Information, and the Synergetic Innovation Center of Quantum Information and Quantum Physics, University of Science and Technology of China, Hefei, Anhui, 230026, China (e-mail of X. Zhou: xizhou@ustc.edu.cn).

capacity of the TES. Such temperature variation is recovered with a response time [15] expressed by

$$\tau_{eff} = \tau_{th}\left[1+\frac{\alpha}{n}\left(1-\frac{T_b^n}{T_c^n}\right)^{-1}\right] \quad (1)$$

where $\tau_{th} = C_e/G$ is the intrinsic thermal recovery time, G is the dominant thermal conductance, n is the exponent of the power law of G, α is the logarithmic derivative of the TES resistance with temperature and T_b is the bath temperature. In the limit of perfect voltage bias, strong electro-thermal feedback, bath temperature $T_b \ll T_c$ and in small signal approximation, τ_{eff} can be described by

$$\tau_{eff} \approx \frac{n}{\alpha}\tau_{th} \approx \frac{C_e}{G} \propto T_c^{-3} \quad (2)$$

where τ_{eff} strongly depends on T_c. In order to reduce the detector recovery time, it is necessary to work at higher temperatures. On the other hand, increasing the device critical temperature degrades the energy resolution since:

$$\Delta E \approx \sqrt{4kT_c^2\frac{C_e}{\alpha}\sqrt{\frac{n}{2}}} \propto T_c^{3/2} \quad (3)$$

As a result, by fabricating very small size TESs (less than 5 μm^2) and by taking advantage from the high transition temperature of Ti (~500 mK), we can fabricate detectors with high energy resolution and fast response time, simultaneously. To fabricate such small TESs, Ti films with a thickness of 35 nm were deposited by e-beam in UHV (2×10^{-8} mbar ÷ 5×10^{-9} mbar) system, on Si/SiN (500 nm) substrates. TESs with an active area of 1 μm × 1 μm and 2 μm × 2 μm were then defined by EBL and lift-off of Ti films. The electrodes were fabricated by lift-off of 40 nm sputtered niobium films. Before the Nb deposition, Ti film surface was sputter-cleaned to reduce the contact resistance between Nb and Ti [18].

III. MEASURED AND SIMULATED DC CHARACTERISTICS

By comparing the measured electro-thermal characteristics of the TESs with results of the simulation based on the two-fluid theory, we can investigate the physical mechanism governing the behavior of the small TES devices. Models based on the two-fluid theory have been developed in [19] and [20], along with circuit simulation techniques suitable for investigating and predicting the behavior of TES circuits.

In this work, we use behavioral modeling as described in [20] and Pspice for circuit simulation. Specifically, by examining the TES voltage V_{tes} under different device temperatures T and current I, we can write the IV relation for the TES as [20]

$$V_{tes} = \theta(T-T_c)IR_n + \theta(T_c-T)(I-I_c)(I-I_c)C_RR_n + \theta(T_c-T)\theta(-I-I_c)(I+I_c)C_RR_n \quad (4)$$

where θ is the step function, C_R is the ratio of the TES resistance in the transitional state to its normal resistance R_n, and the temperature-dependent critical current $I_c(T)$ is given by the BCS relation

$$I_c(T) = I_{c0}\left(1-\frac{T}{T_c}\right)^{1.5} \quad (5)$$

where I_{c0} is the 0-temperature critical current. The IV relation in (4) is based on the two-fluid theory and it is applicable under any temperature and TES current. Because of this, it can be used to simulate the behavior of TES circuits even if the TES device is not restricted to the transition region between the superconducting and normal state. As demonstrated in [20], device model based on it allows us to perform simulations beyond the capability of small-signal models such as DC analysis of the circuit and simulation of AC-biased TES circuits. Also, unlike the small-signal model which does not depend on any particular underlying physical mechanism for the TES device, the IV relation in (4) is specifically based on the two-fluid theory. Details of the simulation results are then directly determined by the two-fluid theory. Therefore, how the simulation results compare to experimental data is a good indication for whether the two-fluid theory can be used to describe the behavior of the TES device under investigation. To construct the device model, we first need to know the physical parameters of the TES, such as the critical temperature T_c, the critical current I_{c0} at 0 K, the normal resistance R_n, the heat conduction coefficient K and the corresponding exponent n.

T_c and R_n are determined from the R-T curves measured with a negligibly small bias current. To estimate I_{c0}, we use the superconducting current $I_c(T)$ measured under different bath temperatures and fit the data by the Ginzburg-Landau equation in (5) as shown in Fig. 1.

To estimate the values for K and n, we calculated the dissipated power P_{tes} of the TES under different bath temperatures T_b. In the transition region, P_{tes} is approximately independent of the bias current due to the electro-thermal feedback. Its value is roughly given by:

$$P_{tes} = K(T_C^n - T_b^n) \quad (6)$$

which is used to fit K and n, as shown in Fig. 2.

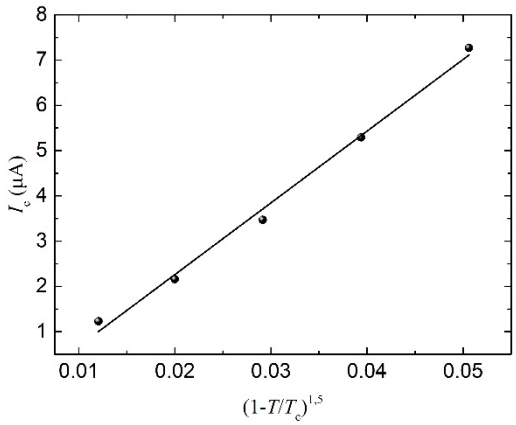

Fig. 1. Critical current of 1 μm × 1 μm TES as a function of $(1-T/T_c)^{1.5}$ (dots) fitted with equation (5) (line) with I_{c0}=158.4 μA.

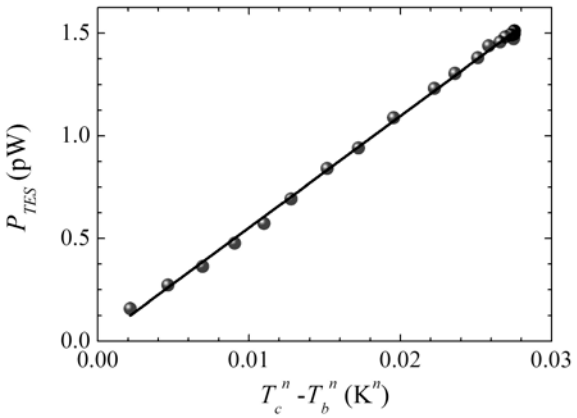

Fig. 2. Quiescent power P_{tes} of 1 μm ×1 μm TES as a function of temperature (dots) fitted with equation (6) (line) with n=4.61, K=5.5×10^{-11}W/K^{n-1} and T_c=0.475 K.

Once the key parameters of the TES, K=5.5×10^{-11}W/K^{n-1} and n=4.61, are determined, we use the TES model based on the two-fluid theory to simulate the bias curve I_{tes} vs. I_b of the TES circuit, as prescribed in [19] and [20], and to compare the results with the measured data. Such values of n and K are in agreement (scaling the area) with those obtained from other Ti-TES deposited on the same substrate but with bigger dimension [21]. Conclusions drawn from such a comparison, both qualitative and quantitative, are a good measure of how well the behavior of our small TES devices is described by the two-fluid theory.

In Fig. 3, the measured and simulated $I_{tes} - I_b$ curves of our 1 μm × 1 μm device are plotted at different bath temperatures for comparison.

As can be seen, the simulated and measured curves are very close numerically, though the deviation becomes more significant when T_b approaches the critical temperature T_c = 475mK. It is also worth noting that both the simulated and measured curves are hysteretic at T_b = 410 mK, 420 mK, and 430 mK, but non-hysteretic at T_b = 440 mK and 450 mK.

The hysteretic behavior is related to different temperatures between the electronic system and the bath. When the material is superconducting these temperatures are close, while in normal state the self-heating increases the electronic temperature. When T_b is close to T_c, the TES bias current is low and its heating effect is negligible. In this case the hysteresis is not present. By lowering T_b the current to keep the TES in its transition grows more and more with a large self-heating effect.

From [22] we know that besides the IV characteristics, also the determination of α and the current sensitivity β is significant to determinate the validity of the two-fluid model. Specially β as a function of R_0/R_n (where R_0 is the TES resistance at the bias point) can fix the region where the two-model fluid is still valid for small device [23]. It is also well known that the best way to obtain α and β is the impedance measurement, but it is very difficult to perform such technique for frequencies higher than 250 kHz [24]. We can only estimate β from the electrical time constant of the single photon pulse $\tau_{el}=L/[R_{sh}+R_0(1+\beta)]$=145 ns [18], where L is the total inductance of the bias circuit, R_0=0.34 Ω and R_{sh}=20 mΩ are the operating and the shunt resistance, respectively. Though it is difficult to accurately estimate L, due to the parasitic inductance, we can estimate β<2 that is much smaller than the limit β=20 @ R_0/R_n=0.05[23]. These observations show that our small TES devices can be described by the two-fluid theory for bath temperatures up to within a few percent from the critical temperature, and TES models developed in [19], [20] can be used to study and predict their behavior. Though weak-link behavior can not ruled out at all, but from [25] a coherent length much smaller than TES side is expected between Nb and Ti at T_c.

IV. Conclusion

In this work, electrical and thermal characterization of TESs as small as 1 μm × 1 μm have been presented. The experimental results have been compared with simulation based on the two-fluids model. Our results have shown that the two-fluid model still works well for our small TES devices.

Acknowledgment

This research receives funding from the European Community's Seventh Framework Programme, ERA-NET Plus, under Grant Agreement No. 912/2009/EC.

This research is supported in part by the China National Natural Science Foundation under grant 11273023 and by the China Central Government University Fundamental Research Fund.

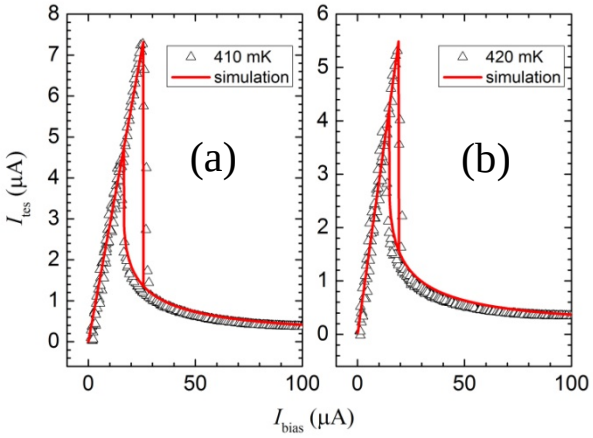

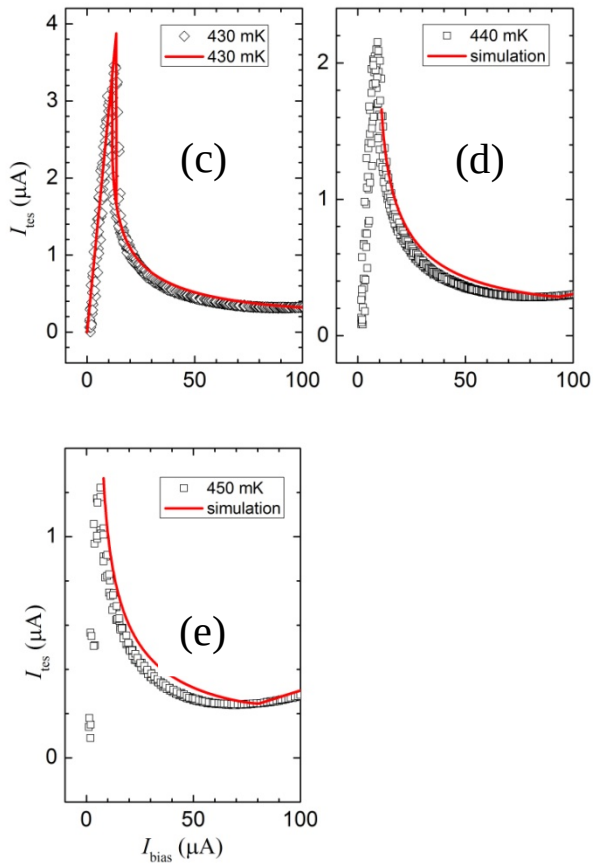

Fig. 3. 1μm×1μmTES current as a function of bias current for different bath temperature (dots) from 410 mK (a) to 450 mK (e) with the corresponding simulation based on two-fluids model (lines).

REFERENCES

[1] S. Takeuchi, "Recent progress in single-photon and entangled-photon generation and applications," *Jpn. J. Appl. Phys.* 53 030101 2014.

[2] A. Ekert, N. Gisin, B. Huttner, H. Inamori, and H. Weinfurter, in *The Physics of Quantum Information*, edited by D. Bouwmeester, A. Ekert, and A. Zelinger (Springer, Berlin, 2000).

[3] J.L. O'Brien, A. Furusawa and J. Vuckovic, "Photonic quantum technologies," *Nat. Photon.* 3 pp. 687-695 2009.

[4] D.A. Bennet, R.D. Horansky, D.R. Schmidt, A.S. Hoover, R. Winkler, B.K. Alpert, J.A. Beall, W.B. Doriese, J.W. Fowler, C.P. Fitzgerald, G.C. Hilton, K.D. Irwin, V. Kotsubo, J.A.B. Mates, G.C. O'Niel, M.W. Rabin, C.D. Reintsema, F.J. Schima, D.S. Swatz, L.R. Vale and J.N. Ullom, "A high resolution gamma-ray spectrometer based on superconducting microcalorimeters," *Rev. Sci. Instrum.* 83 093113 2012

[5] R.D. Horansky, J.N. Ullom, J.A. Beall, G.C. Hilton, K.D. Irwin, L.R. Vale, D. Dry, S.P. Lamont, C.R. Rudy, and M.W. Rabin, "Analysis of nuclear material by alpha spectroscopy with transition-edge microcalorimeter," *J. Low. Temp. Phys.* 151 pp. 1067-1073 2008.

[6] J.C. Zwinkels, E. Ikkonen, N.P. Fox, G. Ulm and M.L. Rastello, "Photometry, radiometry and 'the candela': evolution in the classical and quantum world," *Metrologia* 47 pp. R15-R32 2010.

[7] A. Avella, G. Brida, I.P. Degiovanni, M. Genovese, M. Gramegna, L. Lolli, E. Monticone, C. Portesi, M. Rajteri, M.L. Rastello, E. Taralli, P. Traina, and M. White, "Self consistent, absolute calibration for photon number resolving detectors," *Opt. Exp.* 19 pp. 23249-23257 2011.

[8] C.M. Natarajan, A. Peruzzo, S. Miki, M. Sasaki, Z. Wang, B. Baek, S. Nam, R.H. Hadfield, and J.L. O'Brien, "Operating quantum waveguide circuits with superconducting single-photon detectors," *Appl. Phys. Lett.* 96 211101 2010.

[9] H. Takesue, S.W. Nam, Q. Zhang, R.H. Hadfield, T. Honjo, K. Tamaki and Y. Yamamoto, "Quantum key distribution over a 40-dB channel loss using superconducting single-photon detectors," *Nat. Photon.* 1 343 2007.

[10] J. E. Sadleir, S.J. Smith, S.R. Bandler, J.A. Chervenak, and J.R. Clem, "Longitudinal Proximity Effects in Superconducting Transition-Edge Sensors," *Phys. Rev. Lett.* 104 047003 2010.

[11] A.J. Miller, B. Cabrera, R.M. Clarke, E. Figueroa-Feliciano, , S. Nam and R.W. Romani, "Transition edge sensors as single photon detectors" *IEEE Trans. Appl. Supercond.*9 4205-4208 1999.

[12] D. Fukuda, G. Fujii, T. Numata, A. Yoshizawa, H. Tsuchida, H Fujino, H Ishii, T. Itatani, S. Inoue and T. Zama, "Photon number resolving detection with high speed and high quantum efficiency," *Metrologia*46 S288-S292 2009.

[13] B.S. Karasik, S.V. Pereverzev, A. Soibel, D.F. Santavicca, D.E. Prober, D. Olaya and M.E. Gershenson, "Energy-resolved detection of single infrared photons with λ=8μm using a superconductiongmicrobolometer," *Appl. Phys. Lett.* 101 052601 2012.

[14] C. Portesi, E. Taralli, R. Rocci, M. Rajteri, and M. Monticone, "Fabrication of Au/Ti TESs for optical photon counting," *J. Low Temp. Phys.* 151 261 2008.

[15] L. Lolli, E. Taralli, C. Portesi, E. Monticone, and M. Rajteri, "High intrinsic energy resolution photon number resolving detectors,"*Appl. Phys. Lett.* 103 041107 2013.

[16] L. Lolli, E. Taralli, M. Rajteri, T. Numata, and D. Fukuda, "Characterization of optical fast transition-edge sensors with optimized fiber coupling,"*IEEE Trans. Appl. Supercond.* **23** 2100904 2013.

[17] K.D. Irwin and G.C. Hilton, "Transition edge sensor," in *Cryogenic Particle Detection (Topics Appl. Phys. Vol. 99)*, C. Enss, Ed. Berlin, Germany: Springer-Verlag, 2005, pp.63-149.

[18] C. Portesi, E. Taralli, L. Lolli, M. Rajteri, E. Monticone, "Fabrication and characterization of fast TESs with small area for single photon counting,"*IEEE Trans. Appl. Supercond.*submitted for publication.

[19] T-S. Wang, G-C. Guo, Q-F. Zhu, J-X. Wang, T-F. Li, J-S. Liu, W. Chen, and X. Zhou, "Device modeling of superconductor transition-edge sensors," *IEEE Trans. Appl. Supercond.*, vol 22, 2100212, Aug. 2012.

[20] T-S. Wang, J-K. Chen, Q-Y. Zhang, T-F. Li, J-S. Liu, W. Chen, and X. Zhou, "Simplified two-fluid current-voltage relation for superconductor transition-edge sensors," *Nucl.Instrum. Methods Phys. Res.A, Accel.Spectrom. Detect. Assoc. Equip.*, vol. 729, pp. 474-483, 2013.

[21] D. Fukuda, R. M. T. Damayanthi, A. Yoshizawa, N. Zen, H. Takahashi, K. Amemiya, and M. Ohkubo, "Titanium Based Transition Edge Microcalorimeters for Optical Photon Measurements," *IEEE Trans. Appl. Supercond.*, vol 17, 259, Aug. 2007.

[22] D.A. Bennett · D.S. Swetz · R.D. Horansky ·D.R. Schmidt and · J.N. Ullom, "A Two-Fluid Model for the Transition Shape in Transition-Edge Sensors," *J. Low Temp. Phys.* 167 102-107 2012

[23]D.A. Bennett, D.S. Swetz, D.R. Schmidt, and J.N. Ullom, "Resistance in transition-edge sensors: A comparison of the resistively shunted junction and two-fluid models," *Phys. Rev. B* 87 020508(R) 2013.

[24] E. Taralli, C. Portesi, L. Lolli, E. Monticone, M. Rajteri, I. Novikov and J. Beyer "Impedance measurements on a fast transition-edge sensor for optical and near-infrared range," *Supercond. Sci. Technol.* 23 105012 2010.

[25] A.V. Sergeev, V.V. Mitin, B.S. Karasik, M.E. Gerhenson, "Superconducting nanosensors with mesoscopic number of quasiparticles," *Physica E* 19 173–177 2003.